

Pulsatile flow of viscous and viscoelastic fluids in constricted tubes[†]

A. Javadzadegan^{1,*}, M. Esmaili¹, S. Majidi¹ and B. Fakhimghanbarzadeh²

¹*Department of Mechanical Engineering, University of Tehran, Tehran, Iran*

²*Department of Mechanical Engineering, Sharif University of Technology, Tehran, Iran*

(Manuscript Received December 15, 2008; Revised April 25, 2009; Accepted May 5, 2009)

Abstract

The unsteady flow of blood through stenosed artery, driven by an oscillatory pressure gradient, is studied. An appropriate shape of the time-dependent stenoses which are overlapped in the realm of the formation of arterial narrowing is constructed mathematically. A mathematical model is developed by treating blood as a non-Newtonian fluid characterized by the Oldroyd-B and Cross models. A numerical scheme has been used to solve the unsteady nonlinear Navier-stokes equations in cylindrical coordinate system governing flow, assuming axial symmetry under laminar flow condition so that the problem effectively becomes two-dimensional. Finite difference technique was used to investigate the effects of parameters such as pulsatility, non-Newtonian properties and the flow time on the velocity components, the rate of flow, and the wall shear stress through their graphical representations quantitatively at the end of the paper in order to validate the applicability of the present improved mathematical model under consideration.

Keywords: Cross model; Oldroyd-B model; Pulsatile; Stenoses

1. Introduction

In the arterial system of humans or animals, it is quite common to find localized narrowings, commonly referred to as stenoses, caused by intravascular plaques. There has been great interest in recent years in using numerical methods to study blood flow in stenotic arteries to obtain useful information which may lead to early detection, prevention and diagnosis of various cardiovascular diseases. Such studies are of particular importance because there is indirect evidence that the cause and the development of many cardiovascular diseases are, to a great extent, related to the characteristics of blood flow, such as the high values of the shear stress at the wall or its variation [1, 2]. In most of the investigations relevant to the domain under discussion, the flow is mainly considered in cylindrical pipes of uniform cross-section. But, it is

well known that blood vessels bifurcate at frequent intervals and the diameter of the vessels varies with the distance as propounded by Whitmore [3]. Hence the concept of flow in a varying cross-section forms the prime basis of a large class of problems in understanding blood flow. Manton [4] and Porenta et al. [5] pointed out that most of the vessels could be considered as long and narrow, slowly tapering cones. Numerous investigators have cited hydrodynamic factors playing an important role in the formation of stenosis and hence the mathematical modeling of blood flow through a stenosed tube is very important [6]. Though a great effort has been invested in steady flows [7], very little is known, however, about blood rheology in unsteady flows. Actually, in a living body the heart generates a pulsatile flow and its fluctuations are progressively damped owing to the elasticity of the major arteries; however, the periodic nature of the blood flow is observed in smaller vessels and arterioles where the distensibility of the walls is much less and the influence of pulsation frequency becomes more important. Walls of such vessels can be considered

[†] This paper was recommended for publication in revised form by Associate Editor Yang Na

*Corresponding author. Tel.: +98 21 88251737, Fax.: +98 21 88251737
E-mail address: a.javadzadegan@gmail.com

© KSME & Springer 2009

sufficiently rigid and the flow will be solely determined by the pressure gradient [1]. Many authors have dealt with this problem by treating blood as a Newtonian fluid and assuming the flow to be steady [8]. The Newtonian behavior may be true in larger arteries, but blood, being a suspension of cells in plasma, exhibits non-Newtonian behavior at low shear rates in small arteries [6]. Chaturani and Palanisamy [9] studied the pulsatile flow of blood through rigid tube under the influence of body acceleration. Chaturani and Isaac [10] re-examined the study of Sud and Sekhon [11] and obtained an exact analytical solution of flow variables as functions of real variables. All these studies were restricted to considering blood as a Newtonian fluid, although it is well known from a number of experimental observations that, in most cases, blood behaves as a non-Newtonian fluid. Shukla et al. [12] and Chaturani and Ponnalagar Samy [13] have studied the non-Newtonian behavior for steady flows in stenosed tubes. Therefore, it is of considerable interest to address some essential issues, i.e., the effect of non-Newtonian characteristics on unsteady pulsatile behavior of the flowing blood where the shear-thinning characteristics and viscoelastic property of the non-Newtonian model have been duly accounted for. The purpose of this work is to simulate the behavior of two mathematical models for blood as cross fluid and Oldroyd-B fluid in an artery with partial constriction.

2. Governing equations

The segment of the stenosed artery under consideration is simulated as a thin flexible cylindrical tube containing a non-Newtonian fluid representing the flowing blood. Let (r, θ, z) be the coordinates of a material point in the cylindrical polar coordinate system where the z-axis is taken along the axis of the artery while r, θ are taken along the radial and the circumferential directions, respectively. Let us consider the blood flow through the arterial segment to be nonlinear, laminar and two dimensional, where blood is treated to be an incompressible non-Newtonian fluid. The Navier-Stokes equations and the equation of the continuity that govern the motion of blood may be written in the cylindrical coordinate system as:

$$\frac{\partial V_z}{\partial t} + V_r \frac{\partial V_z}{\partial r} + V_z \frac{\partial V_z}{\partial z} = -\frac{1}{\rho} \frac{\partial P}{\partial z} + \frac{1}{\rho} \left[\frac{1}{r} \frac{\partial}{\partial r} (r \tau_{rz}) + \frac{\partial}{\partial z} (\tau_{zz}) \right] \tag{1}$$

$$\frac{\partial V_r}{\partial t} + V_r \frac{\partial V_r}{\partial r} + V_z \frac{\partial V_r}{\partial z} = -\frac{1}{\rho} \frac{\partial P}{\partial r} + \frac{1}{\rho} \left[\frac{1}{r} \frac{\partial}{\partial r} (r \tau_{rr}) + \frac{\partial}{\partial z} (\tau_{rz}) \right] \tag{2}$$

$$\frac{\partial V_r}{\partial r} + \frac{V_r}{r} + \frac{\partial V_z}{\partial z} = 0 \tag{3}$$

In the cardiovascular system, the motion of the blood is driven by a local pressure gradient along the longitudinal direction of the vessel, which in turn is determined by the propagation of the heart pressure pulse. It is worth noting that the pressure, being essentially periodic, can be subjected to Fourier series analysis. Therefore, for the sake of simplicity, it is assumed that the pressure gradient is known as a function of time [1, 2, and 14]:

$$-\frac{\partial P}{\partial z} = A \cos(\omega_p t) \tag{4}$$

where A is the amplitude of its oscillatory part, $\omega_p = 2\pi f_p$, f_p , being the heart pulse frequency.

2.1 Shear thinning behavior of blood

Investigation of rheological characteristics of blood flow is a very important and controversial subject. It is worth mentioning that blood is a complex fluid whose flow properties are significantly affected by the arrangement, orientation and deformability of red blood cells. At sufficiently low shear rates (smaller than 10 s^{-1}) RBCs (red blood cells) tend to aggregate attaching side-by-side and forming long clusters called rouleaux. If shear rate is decreased even further, to 1 s^{-1} , the rouleaux form long column-like structures, inducing an additional increase of the viscosity. If shear rate is increased, and is high enough, the rouleaux break up, RBCs deform into an infinite variety of shapes without changing volume, and they align with the flow field and tend to slide upon plasma layers formed in between. This induces a decrease of the blood viscosity. Deformability, orientation and aggregation of red blood cells result in shear-thinning viscosity of blood [15]. In the 1960s, attempts to recognize the shear-thinning nature of blood were initiated by Chien et al. [16]. Empirical models like the power-law, Cross [17], Carreau [18], models were seen to agree well in their predictions and were preferred over the power-law model which has an unbounded viscosity at zero shear-rate.

In the present study, the shear thinning behavior of blood is simulated by the Cross model. For this particular constitutive equation, we have [2]:

$$\tau_{zz} = 2 \left\{ \eta_{\infty} + \frac{(\eta_0 - \eta_{\infty})}{1 + (K \dot{\gamma})^{1-n}} \right\} \left(\frac{\partial V_z}{\partial z} \right) \quad (5)$$

$$\tau_{rz} = \left\{ \eta_{\infty} + \frac{(\eta_0 - \eta_{\infty})}{1 + (K \dot{\gamma})^{1-n}} \right\} \left(\frac{\partial V_z}{\partial r} + \frac{\partial V_r}{\partial z} \right), \quad (6)$$

$$\tau_{rr} = 2 \left\{ \eta_{\infty} + \frac{(\eta_0 - \eta_{\infty})}{1 + (K \dot{\gamma})^{1-n}} \right\} \left(\frac{\partial V_r}{\partial r} \right), \quad (7)$$

$$\dot{\gamma} = \left[\left(\frac{\partial V_r}{\partial r} \right)^2 + \left(\frac{\partial V_z}{\partial z} \right)^2 + \left(\frac{V_r}{r} \right)^2 \right]^{\frac{1}{2}} + \left[\left(\frac{\partial V_z}{\partial r} + \frac{\partial V_r}{\partial z} \right)^2 \right]^{\frac{1}{2}}, \quad (8)$$

where $\dot{\gamma}$ is the symmetric rate of deformation tensor. In this model the constants η_0, η_{∞} are the asymptotic viscosities at zero and infinity shear rates:

$$\eta_0 = \lim_{\dot{\gamma} \rightarrow 0} \eta(\dot{\gamma}), \quad \eta_{\infty} = \lim_{\dot{\gamma} \rightarrow \infty} \eta(\dot{\gamma})$$

n is the power index and K are parameters determined by numerical fitting of experimental data.

Table 1 summarizes some of the most common generalized Newtonian models that have been considered for the shear-dependent viscosity of whole human blood with the constant parameters of these models (see Sequeira and Janela [15]).

In Fig. 1 the viscosity of the Cross model for different values of the shear rate is compared with the blood viscosity [19]. From this figure, it can be seen that the four parameter Cross model can predict the shear thinning behavior of blood reasonably well.

2.2 Viscoelastic behavior of blood

Viscoelasticity is a rheological parameter that describes the flow properties of complex fluids like blood. There are two components to the viscoelasticity, the viscosity and the elasticity. The viscosity is related to the energy dissipated during flow primarily

Table 1. Comparison of various non-Newtonian models for blood.

Model	Non-Newtonian Viscosity	Model constant for blood
Power-Law	$\eta(\dot{\gamma}) = K \dot{\gamma}^{n-1}$	$n = 0.61$ $K = 0.42$
Cross	$\eta = \eta_{\infty} + \frac{\eta_0 - \eta_{\infty}}{1 + (K \dot{\gamma})^{1-n}}$	$\eta_0 = 0.056 \text{ Pa.s}$ $\eta_{\infty} = 0.00345 \text{ Pa.s}$ $n = 0.285$ $k = 1.007 \text{ s}$
Carreau	$\eta = \eta_{\infty} + \frac{\eta_0 - \eta_{\infty}}{\left(1 + (K \dot{\gamma})^2\right)^{\frac{1-n}{2}}}$	$\eta_0 = 0.056 \text{ Pa.s}$ $\eta_{\infty} = 0.00345 \text{ Pa.s}$ $n = 0.3568$ $k = 3.313 \text{ s}$

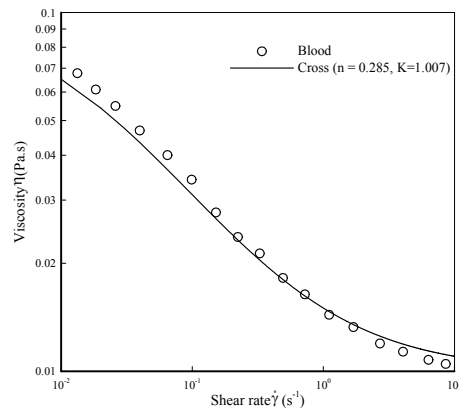


Fig. 1. Viscosity of blood and Cross model versus different values of shear rate.

due to sliding and deformation of red blood cells and red blood cell aggregates. The elasticity is related to the energy stored during flow due to orientation and deformation of red blood cells. Since blood cells are essentially elastic membranes filled with a fluid, it seems reasonable, at least under certain flow conditions, to expect blood to behave like a viscoelastic fluid. At low shear rates RBCs aggregate and are ‘solid-like’, being able to store elastic energy that accounts for the memory effects in blood. At high shear rates, the RBCs disaggregate, forming smaller rouleaux, and later individual cells that are characterized by distinct relaxation times. RBCs become ‘fluid-like’, losing their ability to store elastic energy and the dissipation is primarily due to the internal friction [15]. Thurston (see [20]) was among the earliest to recognize the viscoelastic nature of blood and that the viscoelastic behavior is less prominent with increasing shear rate. Phillips and Deutsch [21] pro-

posed a three-dimensional frame invariant Oldroyd-B type model with four constants. Yelesvarapu [22] has obtained a three constant generalized Oldroyd-B model by fitting experimental data in one-dimensional flows and generalizing such curve fits to three dimensions. They showed that an Oldroyd-B type of model can capture the viscoelastic characteristics of blood well.

In the present study, the viscoelastic behavior of blood is simulated by Oldroyd-B model. For this particular constitutive equation, we have [1]:

$$\tau_{zz} + \lambda_1 \left(\frac{\partial \tau_{zz}}{\partial t} + V_r \frac{\partial \tau_{zz}}{\partial r} + V_z \frac{\partial \tau_{zz}}{\partial z} - 2\tau_{zz} \frac{\partial V_z}{\partial z} - 2\tau_{rz} \frac{\partial V_z}{\partial r} \right) = 2\mu \left(\frac{\partial V_z}{\partial z} \right) \tag{9}$$

$$+ 2\mu\lambda_2 \left(\frac{\partial^2 V_z}{\partial t \partial z} + V_r \frac{\partial^2 V_z}{\partial r \partial z} + V_z \frac{\partial^2 V_z}{\partial z^2} - \left(\frac{\partial V_r}{\partial z} + \frac{\partial V_z}{\partial r} \right) \frac{\partial V_z}{\partial r} - 2 \left(\frac{\partial V_z}{\partial z} \right)^2 \right)$$

$$\tau_{rz} + \lambda_1 \left(\frac{\partial \tau_{rz}}{\partial t} + V_r \frac{\partial \tau_{rz}}{\partial r} + V_z \frac{\partial \tau_{rz}}{\partial z} + \frac{V_r}{r} \tau_{rz} - \tau_{rr} \frac{\partial V_z}{\partial r} - \tau_{zz} \frac{\partial V_r}{\partial z} \right) = \mu \left(\frac{\partial V_z}{\partial r} + \frac{\partial V_r}{\partial z} \right)$$

$$+ \mu\lambda_2 \left(\frac{\partial^2 V_r}{\partial t \partial z} + \frac{\partial^2 V_z}{\partial t \partial r} + V_r \frac{\partial^2 V_r}{\partial r \partial z} + V_z \frac{\partial^2 V_r}{\partial z^2} + V_z \frac{\partial^2 V_z}{\partial r \partial z} + \left[\frac{\partial V_z}{\partial r} + \frac{\partial V_r}{\partial z} \right] \left(\frac{V_r}{r} \right) \right) \tag{10}$$

$$- 2\mu\lambda_2 \left(\frac{\partial V_r}{\partial z} \frac{\partial V_z}{\partial z} + \frac{\partial V_r}{\partial r} \frac{\partial V_z}{\partial r} \right)$$

$$\tau_{rr} + \lambda_1 \left(\frac{\partial \tau_{rr}}{\partial t} + V_r \frac{\partial \tau_{rr}}{\partial r} + V_z \frac{\partial \tau_{rr}}{\partial z} - 2\tau_{rr} \frac{\partial V_r}{\partial r} - 2\tau_{rz} \frac{\partial V_r}{\partial z} \right) = 2\mu \left(\frac{\partial V_r}{\partial r} \right) \tag{11}$$

$$+ 2\mu\lambda_2 \left(\frac{\partial^2 V_r}{\partial t \partial r} + V_z \frac{\partial^2 V_r}{\partial r \partial z} + V_r \frac{\partial^2 V_r}{\partial r^2} - \left(\frac{\partial V_r}{\partial z} + \frac{\partial V_z}{\partial r} \right) \frac{\partial V_r}{\partial z} - 2 \left(\frac{\partial V_r}{\partial r} \right)^2 \right)$$

The constant $\lambda_1 > 0$ is the stress relaxation time (the larger is λ_1 , the slower is relaxation) and λ_2 is the retardation time, with $0 \leq \lambda_2 < \lambda_1$. The material constant μ is the (zero shear rate) viscosity coefficient. The

limit case $\lambda_1 > 0, \lambda_2 = 0$ corresponds to a purely elastic fluid (upper-convected Maxwell fluid), while the limit case $\lambda_1 = \lambda_2 = 0$ corresponds to a purely viscous (Newtonian) fluid with viscosity μ .

2.3 Time dependent geometry of problem

The time-dependent geometry of the stenoses present in the arterial lumen is shown schematically in Fig. 2 and is described mathematically by [23]:

$$\begin{aligned} & \text{for } d \leq z \leq d + l_0 \\ R(z,t) &= \left[r_0 - \frac{4\tau_m(z-d)}{l_0^2} \{l_0 - (z-d)\} \right] a_1(t) \tag{12} \\ & \text{for } z < d, z > d + l_0 \\ R(z,t) &= r_0 a_1(t) \end{aligned}$$

where $R(z,t)$ denotes the radius of the tapered arterial segment in the stenotic region, a the constant radius of the non-tapered artery in the non-stenotic region, l_0 , the length of the stenosis, d , the location of the stenosis and τ_m is taken to be the critical height of the stenosis. The time variant parameter $a_1(t)$ is given by:

$$a_1(t) = 1 - b(\cos \omega t - 1) \exp(-b\omega t) \tag{13}$$

where b is a constant. It is reasonable and convenient to assume that the pressure is independent of the radial coordinate (see Pedley [24]).

2.4 Dimensionless form of governing equations

To make the equations dimensionless we have defined new variables as:

$$\begin{aligned} r &\rightarrow \frac{r}{a}, z \rightarrow \frac{z}{a}, t \rightarrow \frac{Ut}{a}, p \rightarrow \frac{p}{\rho U^2}, \\ V_z &\rightarrow \frac{V_z}{U}, V_r \rightarrow \frac{V_r}{U}, \tau_{rz} \rightarrow \frac{\tau_{rz}}{\rho U^2}, \tau_{zz} \rightarrow \frac{\tau_{zz}}{\rho U^2}, \\ \varepsilon &= \frac{\eta_\infty}{\eta_0} \tau_{rr} \rightarrow \frac{\tau_{rr}}{\rho U^2}, K \rightarrow \frac{KU}{a}, A \rightarrow \frac{A}{U^2} a, \\ \omega &\rightarrow \frac{\omega}{U} a, \lambda_1 \rightarrow \frac{\lambda_1 U}{a}, \lambda_2 \rightarrow \frac{\lambda_2 U}{a}, \text{Re} = \frac{\rho a U}{\mu} \end{aligned} \tag{14}$$

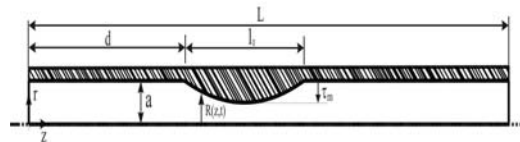


Fig. 2. Schematic diagram of the constricted tube.

where U is a characteristic velocity. The momentum and the continuity equations with the above transformation rewritten, respectively, as:

$$\frac{\partial V_z}{\partial t} + V_r \frac{\partial V_z}{\partial r} + V_z \frac{\partial V_z}{\partial z} = -\frac{\partial P}{\partial z} + \left[\frac{1}{r} \frac{\partial}{\partial r} (r\tau_{rz}) + \frac{\partial}{\partial z} (\tau_{zz}) \right] \tag{15}$$

$$\frac{\partial V_r}{\partial t} + V_r \frac{\partial V_r}{\partial r} + V_z \frac{\partial V_r}{\partial z} = -\frac{\partial P}{\partial r} + \left[\frac{1}{r} \frac{\partial}{\partial r} (r\tau_{rr}) + \frac{\partial}{\partial z} (\tau_{rz}) \right] \tag{16}$$

$$\frac{\partial V_r}{\partial r} + \frac{V_r}{r} + \frac{\partial V_z}{\partial z} = 0 \tag{17}$$

For the Cross model, the stress components are non-dimensionalized as:

$$\bar{\eta} = \left\{ \varepsilon + \frac{(1-\varepsilon)}{1 + \left[K \left[\left(\frac{\partial V_r}{\partial r} \right)^2 + \left(\frac{\partial V_z}{\partial z} \right)^2 + \left(\frac{V_r}{r} \right)^2 + \left(\frac{\partial V_z}{\partial r} + \frac{\partial V_r}{\partial z} \right)^2 \right]^{\frac{1}{2}}} \right\}^{1-n} \tag{18}$$

$$\tau_{rz} = \frac{\bar{\eta}}{\text{Re}} \left(\frac{\partial V_z}{\partial r} + \frac{\partial V_r}{\partial z} \right) \tag{19}$$

$$\tau_{zz} = \frac{2}{\text{Re}} \bar{\eta} \left(\frac{\partial V_z}{\partial z} \right) \tag{20}$$

$$\tau_{rr} = \frac{2}{\text{Re}} \bar{\eta} \left(\frac{\partial V_r}{\partial r} \right) \tag{21}$$

By the non-dimensional parameters, are introduced in Eq. (14), we obtain the following relations for the constitutive equations of the Oldroyd-B model.

$$\tau_{zz} + \lambda_1 \left(\frac{\partial \tau_{zz}}{\partial t} + V_r \frac{\partial \tau_{zz}}{\partial r} + V_z \frac{\partial \tau_{zz}}{\partial z} + \frac{V_r}{r} \tau_{zz} - \tau_{zz} \frac{\partial V_r}{\partial z} \right) = \frac{1}{\text{Re}} \left(\frac{\partial V_z}{\partial r} + \frac{\partial V_r}{\partial z} \right)$$

$$\begin{aligned} & + \frac{1}{\text{Re}} \lambda_2 \left(\frac{\partial^2 V_r}{\partial t \partial z} + \frac{\partial^2 V_z}{\partial t \partial r} + V_r \frac{\partial^2 V_r}{\partial r \partial z} + V_r \frac{\partial^2 V_z}{\partial r^2} \right) \\ & - 2 \frac{1}{\text{Re}} \lambda_2 \left(\frac{\partial V_r}{\partial z} \frac{\partial V_z}{\partial z} + \frac{\partial V_r}{\partial r} \frac{\partial V_z}{\partial r} \right) \\ & + \frac{1}{\text{Re}} \lambda_2 \left(V_z \frac{\partial^2 V_r}{\partial z^2} + V_z \frac{\partial^2 V_z}{\partial r \partial z} + \left[\frac{\partial V_z}{\partial r} + \frac{\partial V_r}{\partial z} \right] \left(\frac{V_r}{r} \right) \right) \end{aligned} \tag{22}$$

$$\tau_{rr} + \lambda_1 \left(\frac{\partial \tau_{rr}}{\partial t} + V_r \frac{\partial \tau_{rr}}{\partial r} + V_z \frac{\partial \tau_{rr}}{\partial z} - 2\tau_{rr} \frac{\partial V_r}{\partial r} - 2\tau_{rz} \frac{\partial V_r}{\partial z} \right) = 2 \frac{1}{\text{Re}} \left(\frac{\partial V_r}{\partial r} \right) \tag{23}$$

$$+ 2 \frac{1}{\text{Re}} \lambda_2 \left(\frac{\partial^2 V_r}{\partial t \partial r} + V_z \frac{\partial^2 V_r}{\partial r \partial z} - 2 \left(\frac{\partial V_r}{\partial r} \right)^2 + V_r \frac{\partial^2 V_z}{\partial r^2} - \left(\frac{\partial V_r}{\partial z} + \frac{\partial V_z}{\partial r} \right) \frac{\partial V_r}{\partial z} \right)$$

$$\tau_{zz} + \lambda_1 \left(\frac{\partial \tau_{zz}}{\partial t} + V_r \frac{\partial \tau_{zz}}{\partial r} + V_z \frac{\partial \tau_{zz}}{\partial z} - 2\tau_{zz} \frac{\partial V_z}{\partial z} - 2\tau_{rz} \frac{\partial V_z}{\partial r} \right) = 2 \frac{1}{\text{Re}} \left(\frac{\partial V_z}{\partial z} \right) \tag{24}$$

$$+ 2 \frac{1}{\text{Re}} \lambda_2 \left(\frac{\partial^2 V_z}{\partial t \partial z} + V_r \frac{\partial^2 V_z}{\partial r \partial z} - 2 \left(\frac{\partial V_z}{\partial z} \right)^2 + V_z \frac{\partial^2 V_z}{\partial z^2} - \left(\frac{\partial V_r}{\partial z} + \frac{\partial V_z}{\partial r} \right) \frac{\partial V_z}{\partial r} \right)$$

2.5 Transformation of the governing equations

The solution scheme used in the present work starts with the transformation below:

$$x = \frac{r}{R(z,t)} \tag{25}$$

Using this transformation, we rewrite the Eqs. (15-24), given by:

$$\begin{aligned} \frac{\partial V_z}{\partial t} = & \left\{ \frac{x}{R} \frac{\partial R}{\partial t} - \frac{V_r}{R} + \frac{x}{R} \frac{\partial R}{\partial z} V_z \right\} \frac{\partial V_z}{\partial x} \\ & - \frac{\partial P}{\partial z} - V_z \frac{\partial V_z}{\partial z} + \left\{ \frac{1}{xR} \tau_{xz} + \frac{1}{R} \frac{\partial \tau_{xz}}{\partial x} \right. \\ & \left. - \frac{\partial \tau_{zz}}{\partial z} + \frac{x}{R} \frac{\partial R}{\partial z} \frac{\partial \tau_{zz}}{\partial x} \right\} \end{aligned} \tag{26}$$

$$\frac{\partial V_r}{\partial t} = \left\{ \frac{x}{R} \frac{\partial R}{\partial t} - \frac{V_r}{R} + \frac{x}{R} \frac{\partial R}{\partial z} V_z \right\} \frac{\partial V_r}{\partial x} - V_z \frac{\partial V_r}{\partial z} + \left\{ \frac{1}{xR} \tau_{xx} + \frac{1}{R} \frac{\partial \tau_{xx}}{\partial x} \right. \\ \left. - \frac{\partial \tau_{xz}}{\partial z} + \frac{x}{R} \frac{\partial R}{\partial z} \frac{\partial \tau_{xz}}{\partial x} \right\} \quad (27)$$

$$\frac{\partial V_z}{\partial z} + \frac{1}{R(z,t)} \frac{\partial V_r}{\partial x} + \frac{V_r}{xR(z,t)} - \frac{x \partial R(z,t) / \partial z}{R(z,t)} \frac{\partial V_z}{\partial x} = 0 \quad (28)$$

For Cross model:

$$\bar{\eta} = \varepsilon + \frac{(1-\varepsilon)}{\left[1 + K \left(\left[2 \left(-\frac{x}{R} \frac{\partial R}{\partial z} \frac{\partial V_z}{\partial x} + \frac{\partial V_z}{\partial z} \right)^2 \right]^{\frac{1}{2}} + \left(\frac{1}{R} \frac{\partial V_z}{\partial x} + \frac{\partial V_r}{\partial z} \right)^2 + \left(-\frac{x}{R} \frac{\partial R}{\partial z} \frac{\partial V_r}{\partial x} \right)^2 + 2 \left(\frac{1}{R} \frac{\partial V_r}{\partial x} \right)^2 \right]^{1-n}} \right)^{1-n}} \quad (29)$$

$$\tau_{xz} = \frac{\bar{\eta}}{\text{Re}} \left(\frac{1}{R} \frac{\partial V_z}{\partial x} + \frac{\partial V_r}{\partial z} - \frac{x}{R} \frac{\partial R}{\partial z} \frac{\partial V_r}{\partial x} \right) \quad (30)$$

$$\tau_{zz} = \frac{2}{\text{Re}} \bar{\eta} \left(\frac{\partial V_z}{\partial z} - \frac{x}{R} \frac{\partial R}{\partial z} \frac{\partial V_z}{\partial x} \right) \quad (31)$$

$$\tau_{xx} = \frac{2}{\text{Re}} \bar{\eta} \left(\frac{1}{R} \frac{\partial V_r}{\partial x} \right) \quad (32)$$

For Oldroyd-B model:

$$\lambda_1 \left(\frac{\partial \tau_{xx}}{\partial t} \right) + \lambda_1 \left(\frac{V_r}{R(z,t)} - \frac{x \partial R / \partial t}{R(z,t)} \right) \frac{\partial \tau_{xx}}{\partial x} + \lambda_1 \left(V_z \frac{\partial \tau_{xx}}{\partial z} \right) + \tau_{xx} \left(1 - \frac{2\lambda_1}{R(z,t)} \right) = \\ \frac{2\lambda_2}{\text{Re}} \left(\frac{1}{R(z,t)} \frac{\partial^2 V_r}{\partial t \partial x} + \frac{V_z}{R(z,t)} \frac{\partial^2 V_r}{\partial z \partial x} \right) + \frac{2\lambda_2}{\text{Re}} \left(-\frac{1}{R(z,t)} \frac{\partial V_z}{\partial x} \left[\frac{\partial V_r}{\partial z} - \frac{x \partial R / \partial z}{R(z,t)} \frac{\partial V_r}{\partial x} \right] \right) \quad (33)$$

$$+ \frac{2\lambda_2}{\text{Re}} \left(-2 \left(\frac{1}{R(z,t)} \frac{\partial V_r}{\partial x} \right)^2 - \left(\frac{\partial V_r}{\partial z} - \frac{x \partial R / \partial z}{R(z,t)} \frac{\partial V_r}{\partial x} \right)^2 \right) + \frac{\lambda_2}{\text{Re}} \left[A_{xx} \left(\frac{\partial V_r}{\partial x} \right) + B_{xx} \left(\frac{\partial^2 V_r}{\partial x^2} \right) + C_{xx} \left(\frac{\partial V_r}{\partial z} \right) \right]$$

$$\lambda_1 \left(\frac{\partial \tau_{xz}}{\partial t} \right) + \lambda_1 \left(\frac{V_r}{R(z,t)} - \frac{x \partial R / \partial t}{R(z,t)} \right) \frac{\partial \tau_{xz}}{\partial x} - V_z \frac{x \partial R / \partial z}{R(z,t)} \frac{\partial \tau_{xz}}{\partial x}$$

$$+ \lambda_1 \left(V_z \frac{\partial \tau_{xz}}{\partial z} + \left(\frac{V_r}{xR(z,t)} + \frac{1}{\lambda_1} \right) \tau_{xz} \right) =$$

$$\frac{\lambda_2}{\text{Re}} \left[\frac{1}{R(z,t)} \frac{\partial^2 V_z}{\partial t \partial x} + \frac{\partial^2 V_r}{\partial t \partial z} - \frac{x \partial R / \partial z}{R(z,t)} \frac{\partial^2 V_r}{\partial t \partial x} \right]$$

$$- \frac{4\lambda_2}{\text{Re}} \left[\left(\frac{\partial V_r}{\partial z} - \frac{x \partial R / \partial z}{R(z,t)} \frac{\partial V_r}{\partial x} \right) \times \left(\frac{\partial V_z}{\partial z} - \frac{x \partial R / \partial z}{R(z,t)} \frac{\partial V_z}{\partial x} \right) \right]$$

$$\left[\frac{V_z}{R(z,t)} \frac{\partial^2 V_r}{\partial z^2} + \frac{V_z}{R(z,t)} \frac{\partial^2 V_z}{\partial z \partial x} - \frac{2}{R(z,t)} \frac{\partial V_r}{\partial x} \frac{\partial V_z}{\partial x} \right]$$

$$+ \frac{\lambda_2}{\text{Re}} \left\{ A_{xz} \left(\frac{\partial V_r}{\partial x} \right) + B_{xz} \left(\frac{\partial^2 V_r}{\partial x^2} \right) + C_{xz} \left(\frac{\partial V_r}{\partial z} \right) + D_{xz} \left(\frac{\partial V_z}{\partial x} \right) + E_{xz} \left(\frac{\partial^2 V_z}{\partial x^2} \right) + F_{xz} \left(\frac{\partial^2 V_r}{\partial z \partial x} \right) \right\} \quad (34)$$

$$\lambda_1 \left(\frac{\partial \tau_{zz}}{\partial t} \right) + \lambda_1 \left(\frac{V_r}{R(z,t)} - \frac{x \partial R / \partial t}{R(z,t)} \right) \frac{\partial \tau_{zz}}{\partial x} - V_z \frac{x \partial R / \partial z}{R(z,t)} \frac{\partial \tau_{zz}}{\partial x}$$

$$+ \lambda_1 \left(V_z \frac{\partial \tau_{zz}}{\partial z} \right) + \left(1 + \lambda_1 \frac{x \partial R / \partial z}{R(z,t)} \right) \tau_{zz} = \quad (35)$$

$$\frac{2\lambda_2}{\text{Re}} \left(\frac{\partial^2 V_z}{\partial t \partial z} - \frac{x \partial R / \partial z}{R(z,t)} \frac{\partial^2 V_z}{\partial t \partial x} + V_z \frac{\partial^2 V_z}{\partial z^2} \right)$$

$$\begin{aligned}
& + \frac{2\lambda_2}{\text{Re}} \left(\frac{-1}{R(z,t)} \frac{\partial V_z}{\partial x} \left[\frac{\partial V_r}{\partial z} - \frac{x \partial R / \partial z}{R(z,t)} \frac{\partial V_r}{\partial x} \right] \right. \\
& \left. - \frac{4\lambda_2}{\text{Re}} \left(\left(\frac{\partial V_z}{\partial z} - \frac{x \partial R / \partial z}{R(z,t)} \frac{\partial V_z}{\partial x} \right)^2 \right) \right. \\
& \left. + \frac{2\lambda_2}{\text{Re}} \left[A_{zz} \left(\frac{\partial V_z}{\partial x} \right) + B_{zz} \frac{\partial^2 V_z}{\partial x^2} \right. \right. \\
& \left. \left. + C_{zz} \left(\frac{\partial^2 V_z}{\partial z \partial x} \right) + D_{zz} \left(\frac{\partial V_z}{\partial z} \right) \right] \right)
\end{aligned}$$

where the expressions of coefficients $A_{xz}, B_{xz}, C_{xz}, D_{xz}, E_{xz}, F_{xz}$ of Eq. (33), A_{xx}, B_{xx}, C_{xx} of Eq. (34) and $A_{zz}, B_{zz}, C_{zz}, D_{zz}$ of Eq. (35) are included in the Appendix for the sake of brevity.

2.6 Boundary condition

Boundary conditions are required for the dependent variables at the boundary faces of the computational domain. At the inlet section located far upstream of the constriction region, the streamwise velocity component and the shear and the normal stress components were set equal to fully developed values and all other quantities were set to zero. The outlet boundary face was located far from the constriction region and the streamwise gradient for velocity and stress could be safely set to zero. Due to symmetry, only half of the physical domain was selected for calculations, and boundary condition on the axis can be taken as:

$$\begin{aligned}
V_r(x, z, t) = 0, \quad \frac{\partial V_z}{\partial x} = 0, \quad \text{on } x = 0 \\
\frac{\partial \tau_{rx}}{\partial x} = 0, \quad \frac{\partial \tau_{xz}}{\partial x} = 0, \quad \frac{\partial \tau_{zz}}{\partial x} = 0, \quad \text{on } x = 0
\end{aligned} \quad (36)$$

Because of the time-dependent geometry and no-slip condition on the wall, appropriate boundary condition on the wall for velocity components can be expressed as:

$$V_r(x, z, t) = \frac{\partial R}{\partial t}, \quad V_z(x, z, t) = 0, \quad \text{on } x = 1 \quad (37)$$

Also, boundary condition on the wall for the stress components, are given implicitly by a relation derived from the constitutive equation after equating the convective terms to zero ($V \cdot \nabla \tau = 0$).

3. Solution methodology

The numerical technique used in the present study is based on the finite difference method. The MacKormack algorithm is used to solve Eqs. (26-35) as described in Tannehill [25]. First, the momentum equations (Eqs. (26, 27)), and the constitutive equations for Cross and Oldroyd-B models (Eqs. (29-35)) are solved using the F.T.C.S scheme (forward time-central space), which is first order accurate for time derivations and second order accurate for spatial derivatives. Discretized momentum and constitutive equations lead to algebraic equation systems for velocity components V_r, V_z and stress components $\tau_{rr}, \tau_{rz}, \tau_{zz}$ where the pressure gradient and the fluid properties are taken from the previous iteration except the first iteration where initial conditions are applied. By this way the value of velocity and stress components will be predicted and the predicted velocity and stress fields are then used to solve the velocity-correction and the stress-correction equations using the same equation solver and to the same tolerance. In numerical computations, the results are obtained for different values of the flow characteristics with step size in the z -direction with $\Delta z = 0.05$, in the x -direction $\Delta x = 0.025$ and in the t -direction with $\Delta t = 0.00001$. Further reduction of $\Delta z, \Delta x$, and Δt produces a change in the fifth or sixth decimal places. Hence, the values $\Delta z = 0.05$, $\Delta x = 0.025$ and $\Delta t = 0.00001$ have been maintained throughout the computational work.

4. Numerical results

Once the problem has been formulated in a non-dimensional form and a numerical scheme has been implemented as in the former section, the many parameters have been fixed to some likelihood to the blood flow: some of them are typical of physiological measurements and are chosen to obtain a velocity waveform with characteristic similar to the artery velocity pulses, some others are taken from the literature [1, 2]:

$$\begin{aligned}
a = 0.1 \text{ cm}, \quad \rho = 1.06 \text{ g/cm}^3, \quad L = 25 \text{ cm}, \\
l_0 = 1.6 \text{ cm}, \quad d = 12 \text{ cm}, \quad \tau_m = 0.4 \text{ a}, \quad \varepsilon = 0.06 \\
A = 32500 \text{ g}(\text{cms})^{-2}, \quad f_p = 1.2 \text{ Hz}, \quad U = 1 \text{ cms}^{-1}
\end{aligned} \quad (38)$$

For the purpose of validation, variation of the flow rate through non-constricted artery assuming that

blood is an Oldroyd-B fluid is compared with Pontrelli. [1]. As shown in Fig. 3, the results are found to be in good agreement.

The code developed in this work was solved for the blood flowing through a stenosed artery with two non-Newtonian models.

Fig. 4 shows the variation of the axial velocity of Cross and Oldroyd-B models at midpoint of stenosis at an instant ($t = 0.5$). The curves are all featured to be analogous in the sense that they do decrease from their individual maxima at the axis as one moves away from it and finally drop to zero on the wall surface. Velocity profiles corresponding to Cross model represented higher values than the Oldroyd-B and Newtonian models. As shown in Fig. 4, another point of comparison is the different index parameters (n) for the Cross model. From this figure, one may conclude that as the index parameter (n) increases, the axial velocity profile assumes a flat shape.

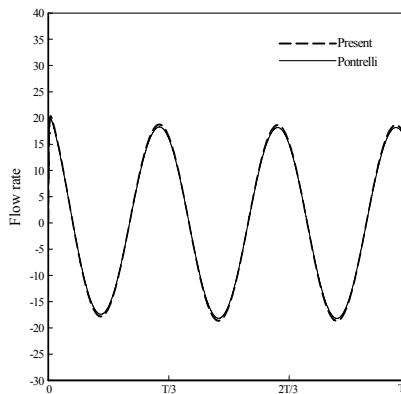


Fig. 3. Comparison of the flow rate.

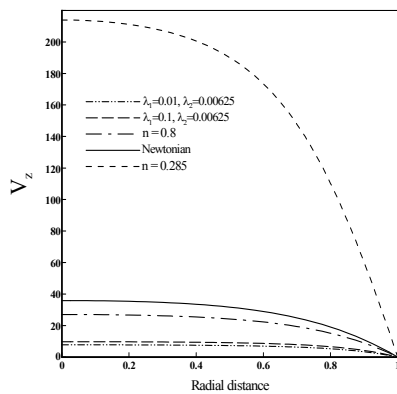


Fig. 4. Radial variation of the axial velocity for Oldroyd-B and Cross models at an instant ($t = 0.5$).

Fig. 5 shows numerical results obtained for the radial velocity component at the same axial location and at the same time step of ($t = 0.5$) for different values of relaxation time (λ_1). Through analysis of Fig. 5, one may note that all curves are found to be increasing from zero on the axis and to attain some negative finite value on the wall surface due to wall motion. If an arterial wall is treated to be rigid, then the radial velocity profile takes an almost symmetrical shape with zero velocity on the wall surface. From this figure it can be seen that the radial velocity profile is affected by the change of the relaxation time value. As expected, the magnitude of the radial velocity is seen to be smaller than the axial velocity.

Fig. 6 shows the profiles for flow rate of the Cross model at midpoint of stenosis for different index parameter (n). One may take note from the present figure that the flow rate diminishes by increasing of

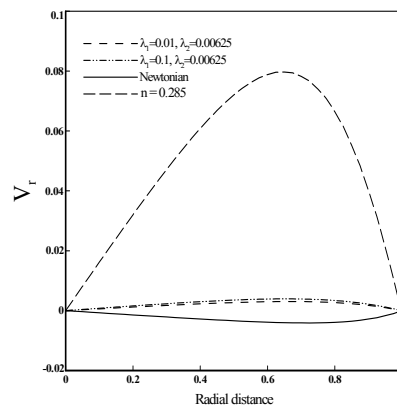


Fig. 5. Radial variation of the radial velocity for Oldroyd-B and Cross models at an instant ($t = 0.5$).

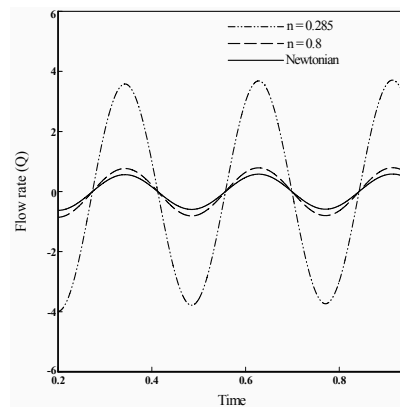


Fig. 6. Variation of rate of flow with time for different values of n .

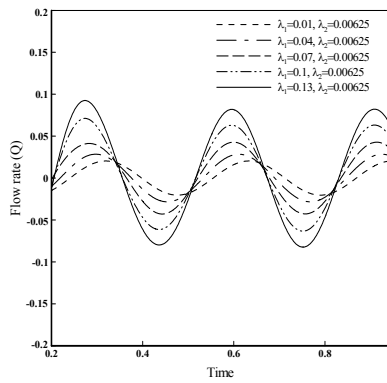


Fig. 7. Variation of the rate of flow with time for different value of λ_1 .

the index parameter (n), and it can be seen that the flow rate profile is strongly affected by the index parameter (n). Studying all the results referred to in the present figure, one may conclude that as the index parameter (n) increases, the Cross model shows similar behavior to the Newtonian model.

Fig. 7 includes more results showing the effect of the relaxation time (λ_1) on the flow rate of the Oldroyd-B model. The deviation of the results thus obtained clearly estimates the effect of relaxation time quantitatively on the flow rate of the Oldroyd-B model. The pulsatile nature of the flow rate has been found to be distributed for all the curves throughout the time scale considered here. Through analyzing of all curves of the present figure, one may conclude that by increasing the relaxation time (λ_1), the flow rate increases considerably. It is quite interesting to note that for the fixed value of the retardation time $\lambda_2 = 0.00625$, as the relaxation time (λ_1) increases, the tendency of flow reversal increases so that for $\lambda_1 = 0.13$, massive back flow for a considerable period of time occurs.

Since the magnitude and the variation of the shear stress at the wall is relevant for the localization and prediction of the disease in blood vessel, the time history in the last two cycle is plotted in Fig. 8. The deviation in results for the Cross model and for the Oldroyd-B model can be visualized and their effects on the stresses from the relevant curves of the present figure can be quantified. As can be seen in this figure, for the Cross model the wall shear stress is higher than that for Oldroyd-B and Newtonian models. From this figure it is obvious that by increasing the index parameter (n) and the relaxation time (λ_1), the wall shear stress increases.

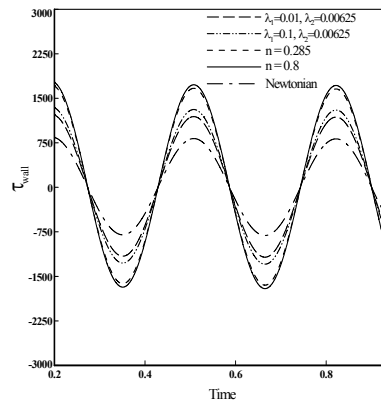


Fig. 8. Distribution of wall shear stress as a function of time for Oldroyd-B and Cross models.

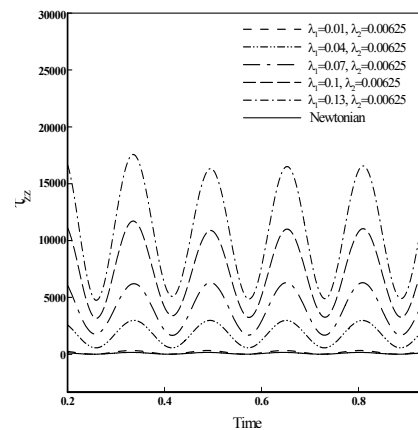


Fig. 9. Distribution of normal stress τ_{zz} as a function of time for Oldroyd-B model.

Variations of the normal stress τ_{zz} with time for different values of the relaxation time (λ_1) at mid-point of stenosis are presented in Fig. 9. It appears that the normal stress is pulsatile throughout the time period under consideration. It is observed that the τ_{zz} can reach an order of magnitude larger than the shear stress and is most sensitive to the variation of relaxation time (λ_1).

Radial distribution of the resultant normal stress (τ_{zz}) is computed at an instant ($t = 0.5$) and illustrated in Fig. 10. The results of the present figure include the effect of relaxation time (λ_1) on the normal stress (τ_{zz}). It is interesting to note that the Newtonian model predicts a smaller value of the normal stress (τ_{zz}) than the Oldroyd-B model, and by increasing the relaxation time (λ_1), the normal stress (τ_{zz}) increases considerably.

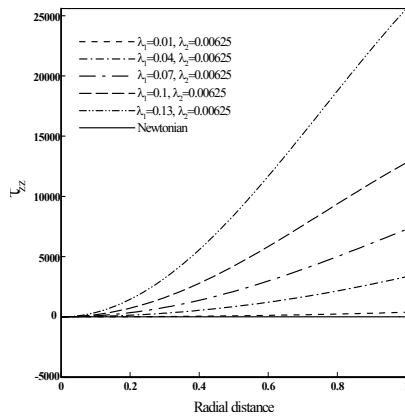


Fig. 10. Radial variation of the normal stress τ_{rr} for different value of λ_1 at an instant ($t = 0.5$).

5. Conclusions

Localized narrowing of an artery is a frequent effect or a cause of vascular diseases. Such constriction disturbs normal blood flow through the vessel, and there is considerable evidence that fluid dynamical factors play a significant role in the development and progression of disease itself. This paper presented numerical results for an unsteady blood flow in an artery with stenosis, using the Cross and Oldroyd-B models of blood viscosity. The results demonstrate that the characteristics of blood flow are affected by the non-Newtonian rheology, in some typical regimes, change the flow pattern; and increase the normal stress and the shear stress at the wall in comparison with the Newtonian model. The differences between the Newtonian and non-Newtonian models show that the non-Newtonian behavior is an important factor and should not be neglected in small blood vessels (smaller than 1 mm).

Acknowledgment

The author would like to thank the Research Council of the University of Tehran (RCUT) for supporting this work.

References

- [1] G. Pontrelli, Pulsatile blood flow in a pipe, *Computers & Fluids*. 27 (1998) 367-380.
- [2] P. K. Mandal, S. Chakravarty, A. Mandal and N. Amin, Effect of body acceleration on unsteady pulsatile flow of non-Newtonian fluid through a stenosed artery, *Applied Mathematics and Computation*. 189 (2007) 766-779.
- [3] R. L. Whitmore, *Rheology of circulation*, Pergamon Press, Oxford, 1968.
- [4] M. J. Manton, Low Reynolds number flow in slowly varying axisymmetric tubes, *J. Fluid Mech.* 49 (1971) 451-459.
- [5] G. Porenta, G. F. Young and T. R. Rogge, A finite element model of blood flow in arteries including taper, branches and obstructions, *J. Biomech. Eng.* 108 (1986) 161-167.
- [6] D. S. Sankar and K. Hemalatha, Pulsatile flow of Herschel-Bulkley fluid through stenosed arteries- A mathematical model, *Non-linear Mechanics*. 41 (2006) 979-990.
- [7] D. L. Fry, Measurements of pulsatile blood flow by the computed pressure gradient technique, *IRE Trans. Med. Electron.* ME-6 (1959) 259-264.
- [8] D. Liepsch, an introduction to biofluid mechanics basis models and application, *J. Biomech.* 35 (2002) 415-435.
- [9] P. Chaturani and V. Palanisamy, Pulsatile flow of blood with periodic body acceleration, *Int. J. Eng. Sci* 29 (1991) 113-121.
- [10] P. Chaturani and Issac A. S. A. Wassf, Blood flow with body acceleration forces, *Int. J. Eng. Sci.* 33 (1995) 1807-1820.
- [11] V. K. Sud and G. S. Sekhon, Arterial flow under periodic body acceleration, *Bull. Math. Biol.* 47 (1985) 35-52.
- [12] J. B. Shukla, R. S. Parihar and S. P. Gupta, Biorheological aspects of blood flow through artery with mild stenosis: effects of peripheral layer, *Biorheology* 17 (1980) 403-410.
- [13] P. Chaturani and R. Ponnalagar Samy, A study of non-Newtonian aspects of blood flow through stenosed arteries and its applications in arterial diseases, *Biorheology* 22 (1985) 521-531.
- [14] A. C. Burton, *Introductory text, In Physiology and Biophysics of the circulation*, Year Book Medical Publisher, Chicago, IL, (1966).
- [15] A. Sequeira and J. Janela, An overview of some mathematical models of blood rheology, *A Portrait of State-of-the-Art Research at the Technical University of Lisbon*, (2007) 65-87.
- [16] S. Chien, S. Usami, R. J. Dellenback and M. I. Gregersen, Blood viscosity: Influence of erythrocyte deformation, *Science* 157 (3790), pp. 827-829.
- [17] M. M. Cross, Rheology of non-Newtonian fluids: a new flow equation for pseudo-plastic systems, *J.*

Colloid Sci., 20, 1965, pp. 417-437.

[18] P. J. Carreau, *PhD Thesis*, University of Wisconsin, Madison, 1968.

[19] C. W. Macosko, *Rheology principles, measurements and applications*, VCH publication (1993).

[20] G. B. Thurston, Viscoelasticity of human blood, *Biorheology* 12 (1972) 1205-1217.

[21] W. M. Phillips and S. Deutsch, Toward a constitutive equation for blood, *Biorheology* 12 (1975) 383-389.

[22] K. K. Yelesvarapu, M. V. Kameneva, K. R. Rajagopal and J. F. Antaki, The flow of blood in tubes: theory and experiment, *Mech. Res. Comm.*, (25) 3, 1998, pp. 257-262.

[23] P. K. Mandal, An unsteady analysis of non-Newtonian blood flow through tapered arteries with stenosis, *Int.J. Non-Linear Mechanics* 40 (2005) 151-164.

[24] T. J. Pedley, *The Fluid mechanics of large blood vessels*, Cambridge University Press, London, 1980.

[25] J. Tannehill, D. Anderson and R. Pletcher, *Computational Fluid Mechanics and Heat Transfer*, Philadelphia 1984.

Appendix

While those of A_{xx} , B_{xx} and C_{xx} of Eq. (33) are of the form given by:

$$A_{xx} = 2 \left(-\frac{\partial R / \partial t}{R(z,t)^2} - \frac{V_z}{R(z,t)^2} \frac{\partial R}{\partial z} \right) + \frac{2\lambda_2}{R(z,t)} - \frac{\text{Re} \lambda_1}{\lambda_2} \frac{2x \partial R / \partial z}{R(z,t)} \tag{A1}$$

$$B_{xx} = 2 \left[-\frac{x \partial R / \partial t}{R(z,t)^2} + \frac{V_r}{R(z,t)^2} - V_z \frac{x \partial R / \partial z}{R(z,t)^2} \right] \tag{A2}$$

$$C_{xx} = 2\tau_{xz} \frac{\text{Re} \lambda_1}{\lambda_2} \tag{A3}$$

The expressions of the coefficients A_{zz} , B_{zz} , C_{zz} , D_{zz} , E_{zz} , F_{zz} of Eq. (34) should be read as:

$$A_{zz} = \frac{3x}{R(z,t)^2} \frac{\partial R}{\partial t} \frac{\partial R}{\partial z} - \frac{x}{R(z,t)} \frac{\partial^2 R}{\partial t \partial z} - V_r \frac{\partial R / \partial z}{R(z,t)^2} - \frac{V_r}{R(z,t)^2} \frac{\partial R}{\partial z} + V_z \left(\frac{3x}{R(z,t)^2} \left(\frac{\partial R}{\partial z} \right)^2 - \frac{x}{R(z,t)} \frac{\partial^2 R}{\partial z^2} \right) \tag{A4}$$

$$- \frac{x \partial R / \partial z}{R(z,t) \lambda_2} - \tau_{zz} \frac{\text{Re} \lambda_1}{\lambda_2} \frac{x \partial R / \partial z}{R(z,t)}$$

$$B_{zz} = \frac{x^2}{R(z,t)^2} \frac{\partial R}{\partial t} \frac{\partial R}{\partial z} - \frac{x V_r}{R(z,t)^2} \frac{\partial R}{\partial z} + \left(\frac{x \partial R / \partial z}{R(z,t)} \right)^2 V_z \tag{A5}$$

$$C_{zz} = \frac{V_r}{xR(z,t)} + \lambda_2 + \tau_{zz} \frac{\text{Re} \lambda_1}{\lambda_2} \tag{A6}$$

$$D_{zz} = -\frac{\partial R / \partial t}{R(z,t)^2} - V_z \frac{\partial R / \partial z}{R(z,t)^2} + \frac{V_r}{xR(z,t)^2} + \frac{1}{R(z,t) \lambda_2} + \frac{\tau_{zz}}{R(z,t)} \frac{\text{Re} \lambda_1}{\lambda_2} \tag{A7}$$

$$E_{zz} = -V_z \frac{x \partial R / \partial z}{R(z,t)^2} - \frac{x \partial R / \partial t}{R(z,t)^2} + \frac{V_r}{R(z,t)^2} \tag{A8}$$

$$F_{zz} = -\frac{x \partial R / \partial t}{R(z,t)} + \frac{V_r}{R(z,t)} - 2 \frac{x \partial R / \partial z}{R(z,t)} V_z \tag{A9}$$

And the expressions of the coefficients A_{zz} , B_{zz} , C_{zz} , D_{zz} of Eq. (35) are given by:

$$A_{zz} = \frac{3x}{R(z,t)^2} \frac{\partial R}{\partial t} \frac{\partial R}{\partial z} - \frac{x}{R(z,t)} \frac{\partial^2 R}{\partial t \partial z} - \frac{V_r}{R(z,t)^2} \frac{\partial R}{\partial z} + V_z \left(\frac{3x}{R(z,t)^2} \left(\frac{\partial R}{\partial z} \right)^2 - \frac{x}{R(z,t)} \frac{\partial^2 R}{\partial z^2} \right) - \lambda_2 \frac{x \partial R / \partial z}{R(z,t)} + \frac{\text{Re} \lambda_1}{\lambda_2} \frac{\tau_{zz}}{R(z,t)} \tag{A10}$$

$$B_{zz} = -\frac{x \partial R / \partial z}{R(z,t)} + V_z \left(\frac{x \partial R / \partial z}{R(z,t)} \right)^2 + \frac{x^2}{R(z,t)^2} \frac{\partial R}{\partial t} \frac{\partial R}{\partial z} \tag{A11}$$

$$C_{zz} = -\frac{x \partial R / \partial t}{R(z,t)} + \frac{V_r}{R(z,t)} - 2 \frac{x \partial R / \partial z}{R(z,t)} V_z \tag{A12}$$

$$D_{zz} = \frac{1}{\lambda_2} \tag{A13}$$



and Biomass.

Ashkan Javadzadegan received his B.S. in Mechanical Engineering from University of Tabriz, Iran, in 2006. He then received his M.S. degree from University of Tehran, Iran in 2008. His research interests include rheology, heat transfer



interests include rheology, heat transfer and porous media.

Sahand Majidi received his B.S. in Mechanical Engineering from Khaje Nasir Toosi University of Technology (K.N.T.U), Tehran, Iran, in 2006. He then received his M.S. degree from the University of Tehran in 2008. His research



University of Technology in 2009. His research interests include Biofluidics, rheology, micro and nanofluidics and MHD flow.

Mostafa Esmaili received his B.S. in Mechanical Engineering from University of Buali Sina Hamadan, Iran, in 2006. He then received his M.S. degree from University of Tehran in 2008. He has been accepted into the Ph.D program at Sharif



Biomass.

Babak Fakhimghanbarzadeh received his B.S. in Mechanical Engineering from University of Tabriz, Iran, in 2006. He then received his M.S. degree from Sharif University of Technology in 2008. His research interests include Exergoeconomics,